

Effective Application of Normalized Min-Sum Decoding for BCH Codes

Guangwen Li, Xiao Yu

Abstract—High-throughput decoding of BCH codes necessitates efficient and parallelizable decoders. However, the algebraic rigidity of BCH codes poses significant challenges to applying parallel belief propagation variants. To address this, we propose a systematic design scheme for constructing parity-check matrices using a heuristic approach. This involves a sequence of binary sum operations and row cyclic shifts on the standard parity-check matrix, aiming to generate a redundant, low-density, and quasi-regular matrix with significantly fewer length-4 cycles. The relationships between frame error rate, rank deficiency of minimum-weight dual-code codewords, and row redundancy are empirically analyzed. For the revised normalized min-sum decoder, we introduce three types of random automorphisms applied to decoder inputs. These are unpacked and aggregated by summing messages after each iteration, achieving a 1-2dB improvement in bit error rate compared to parallelizable counterparts and two orders of magnitude faster convergence in iterations than iterative rivals. Additionally, undetected errors are highlighted as a non-negligible issue for very short BCH codes.

Index Terms—BCH codes, Belief propagation, Min Sum decoding, Code automorphism, Neural network,

I. INTRODUCTION

FOR low-density parity-check (LDPC) codes [1], belief propagation (BP) [2] and its variants dominate decoding due to their asymptotic maximum-likelihood (ML) performance and high data throughput enabled by parallelizable implementations. However, applying BP variants effectively to classical linear block codes with high-density parity-check (HDPC) matrices, such as Bose–Chaudhuri–Hocquenghem (BCH) and Reed–Muller (RM) codes, remains challenging. The inherent abundance of short cycles in their Tanner graphs (TGs) disrupts the assumed message independence required for optimal decoding. This has spurred significant interest within the coding community to develop effective decoding schemes for HDPC codes.

The importance of exploiting code structure to facilitate decoding has long been recognized. Jiang et al. [3] proposed stochastic shifting mechanisms and varied damping coefficients for updated log-likelihood ratios (LLRs) of codeword bits. They further adapted the parity-check matrix (PCM) based on consecutive reliability updates of codeword bits across iterations [4], aiming to prevent BP from stalling in pseudo-equilibrium points. Halford et al. [5] introduced random redundant decoding (RRD), demonstrating improved bit error rate (BER) performance with a cycle-reduced PCM. Ismail et al. [6] suggested permuted BP (PBP), which applies

a randomly chosen automorphism to messages in each BP iteration. Santi et al. [7] incorporated minimum weight parity checks tailored to received sequences, achieving stronger BP decoding over fully redundant PCMs for RM codes at the cost of batch processing capability. Babalola et al. [8] proposed a generalized parity-check transformation (GPT) to update bit reliability using on-the-fly syndrome, although this method suffers from poor BER and lacks parallelizability.

The modified RRD (mRRD) algorithm [9] fixed the damping factor and used multiple parallel decoders based on PCM permutations, offering lower complexity than [10], which employed multiple PCMs composed of cyclic shifts of various minimum weight dual-code codewords. Geiselhart et al. [11] generalized the ensemble decoding strategy by incorporating diverse constituent decoders, achieving near-ML performance for RM codes.

Inspired by the success of deep learning, Nachmani et al. [12] proposed neural BP (NBP), which weights messages passed in TGs. Lian et al. [13] demonstrated that shared parameters tailored to varying signal-to-noise ratios (SNRs) in NBP alleviate complexity without performance loss. Buchberger et al. [14] pruned uninformative check nodes in overcomplete PCMs for NBP. However, the performance improvement of these NBP variants in terms of frame error rate (FER) or BER remains modest relative to their complexity.

Recognizing the critical impact of PCMs on BP performance, Lucas et al. [15] advocated PCMs composed of minimum weight dual-code codewords for their low density of non-zero elements. Yedidia et al. [16] proposed expanding PCMs with auxiliary "bits" to reduce row weight and short cycles. Kou et al. [17] demonstrated that appropriate redundant PCM rows greatly enhance BP decoding of finite LDPC algebraic-geometry codes, inspiring the exploration of similar strategies for HDPC codes.

On the other hand, universal ordered statistics decoding (OSD) [18] variants can decode without leveraging specific code properties. Recently, Bossert et al. [19] employed formation set decoding as an OSD variant for BCH codes, achieving competitive FER performance. However, its serial processing nature suggests its role as an auxiliary method rather than the primary decoder for high-throughput scenarios.

To address challenges such as the nested loops in BP decoding [4], [6], [9], high complexity of ensemble decoding [9], [10], [11], and limited throughput due to Gaussian elimination in PCM processing [7], [8], we propose a revised normalized min-sum (NMS) decoder with domain knowledge of BCH codes, enabled by an optimized PCM. The main contributions are as follows:

G.Li is with Shandong Technology and Business University, Yantai, China
X.Yu is with Binzhou Medical University, Yantai, China.

- * An optimization method to systematically grow a targeted PCM from standard PCM, achieving modest redundancy, cycle reduction, quasi-regularity, and lower density.
- * A revised NMS decoder incorporating multiple automorphisms applied simultaneously to inputs, with aggregated messages significantly expediting NMS decoding.
- * Identification of the impact of rank deficiency in minimum weight dual-code codewords on decoding performance and the non-negligible issue of falsely positive decoding for very short BCH codes.

The remainder of this paper is organized as follows: Section II reviews preliminaries of NMS and mRRD variants. Section III details the PCM optimization method and revised NMS decoder. Section IV presents experimental results and complexity analysis. Concluding remarks are provided in Section V.

II. PRELIMINARIES

Consider a binary message row vector $\mathbf{m} = [m_i]_1^K$, encoded into a codeword $\mathbf{c} = [c_i]_1^N$ using $\mathbf{c} = \mathbf{m}\mathbf{G}$ over the Galois field $\text{GF}(2)$. Here, K and N denote the lengths of the message and codeword, respectively, while \mathbf{G} represents the generator matrix. Each bit c_i is mapped to an antipodal symbol using binary phase-shift keying (BPSK) modulation, given by $s_i = 1 - 2c_i$. Due to additive white Gaussian noise (AWGN) n_i with zero mean and variance σ^2 , the received sequence at the channel output is $\mathbf{y} = [y_i]_1^N$, where $y_i = s_i + n_i$. This sequence is subsequently sent to the decoder for codeword estimation.

The log-likelihood ratio (LLR) $\mathbf{L}(\mathbf{y})$ is derived element-wise, with its i -th component expressed as:

$$L_i = \log \left(\frac{p(y_i | c_i = 0)}{p(y_i | c_i = 1)} \right) = \frac{2y_i}{\sigma^2}. \quad (1)$$

A larger magnitude of y_i reflects higher confidence in the hard decision for the i -th bit, a property leveraged by most OSD variants during decoding. Unlike standard BP decoding, the NMS variant exhibits channel invariance [20], permitting arbitrary evaluation of σ^2 (e.g., setting $\sigma^2 = 2$) without impacting performance.

A. Original NMS

The TG of a code is fully determined by its PCM \mathbf{H} of dimensions $M \times N$, where $M \geq N - K$ when row redundancy is allowed. Variable nodes $v_i, i = 1, 2, \dots, N$, exchange messages with check nodes $c_j, j = 1, 2, \dots, M$, if nonzero entries exist in the j -th row and i -th column of \mathbf{H} .

Under a flooding message schedule in NMS decoding, within the LLR domain, the message from v_i to c_j at the t -th iteration ($t = 1, 2, \dots, I_m$) is computed as:

$$x_{v_i \rightarrow c_j}^{(t)} = L_i + \sum_{\substack{c_k \rightarrow v_i \\ k \in \mathcal{C}(i) \setminus j}} x_{c_k \rightarrow v_i}^{(t-1)}, \quad (2)$$

while the message from c_j to v_i is given by:

$$x_{c_j \rightarrow v_i}^{(t)} = \alpha \cdot \prod_{\substack{v_k \rightarrow c_j \\ k \in \mathcal{V}(j) \setminus i}} \text{sgn} \left(x_{v_k \rightarrow c_j}^{(t)} \right) \cdot \min_{k \in \mathcal{V}(j) \setminus i} \left| x_{v_k \rightarrow c_j}^{(t)} \right|, \quad (3)$$

where the normalization factor α is determined empirically. The set $\mathcal{C}(i) \setminus j$ refers to the indices of all neighboring check nodes of v_i except c_j , and $\mathcal{V}(j) \setminus i$ refers to those of all neighboring variable nodes of c_j except v_i . All terms $x_{c_p \rightarrow v_i}^{(0)}$ in (2) are initialized to zero.

Messages are updated alternately via (2) and (3) along the edges of the TG until the maximum iteration limit I_m is reached. Simultaneously, the output LLRs of codeword bits at the t -th iteration are evaluated as:

$$x_i^{(t)} = L_i + \sum_{\substack{c_k \rightarrow v_i \\ k \in \mathcal{C}(i)}} x_{c_k \rightarrow v_i}^{(t-1)}, \quad (4)$$

from which a tentative hard decision $\hat{\mathbf{c}} = [\hat{c}_i^{(t)}]_1^N$ is derived and verified against the early stopping criterion:

$$\mathbf{H}\hat{\mathbf{c}}^\top = \mathbf{0}. \quad (5)$$

B. mRRD and PBP

Algorithm 1 mRRD decoder [9]

Input: $\mathbf{y}, \mathbf{L}(\mathbf{y}), \mathbf{H}$, automorphism group $\mathbf{P}_g, S = \emptyset$

Output: optimal codeword estimate $\hat{\mathbf{c}}$ for \mathbf{y} .

- 1: **for** $i = 1, 2, \dots, I_3$
 - 2: $\mathbf{w} \leftarrow \mathbf{L}(\mathbf{y})$; pick one ρ from \mathbf{P}_g ; $\mathbf{w} \leftarrow \rho(\mathbf{w})$; $\Theta \leftarrow \rho$
 - 3: **for** $j = 1, 2, \dots, I_2$
 - 4: Perform I_1 BP iterations to yield output \mathbf{w}_o ; $\mathbf{w} \leftarrow \mathbf{w} + \mathbf{w}_o$; compute hard decision $\hat{\mathbf{c}}_i$ on \mathbf{w} .
 - 5: **if** $\mathbf{H}\hat{\mathbf{c}}_i^\top = \mathbf{0}$ $S \leftarrow S \cup i$; apply Θ^{-1} to \mathbf{w} and $\hat{\mathbf{c}}_i$; **break**
 - 6: **else** Draw another ρ from \mathbf{P}_g ; $\mathbf{w} \leftarrow \rho(\mathbf{w})$; $\Theta \leftarrow \rho \cdot \Theta$
 - 7: **if** $S = \emptyset$ $S \leftarrow \{1, 2, \dots, I_3\}$
 - 8: $\hat{\mathbf{c}} = \arg \max_{i \in S} \sum_{k=1}^N |y_k - \hat{c}_{i,k}|^2$.
-

For linear block codes, any permutation $\rho(\cdot)$ satisfies the relation:

$$\rho(\mathbf{H})\hat{\mathbf{c}}^\top = \mathbf{H}(\rho^{-1}(\hat{\mathbf{c}}))^\top. \quad (6)$$

For cyclic BCH codes, automorphisms are specific permutations mapping the code onto itself, with their effect on \mathbf{H} interpretable as inverse permutations on the input data. Consequently, $\rho^{-1}(\mathbf{L}(\mathbf{y}))$ can serve as a surrogate to support soft decoding of $\mathbf{L}(\mathbf{y})$. Accordingly, the mRRD algorithm in Algorithm 1 deploys I_3 decoders in parallel to achieve diversity gain. Random automorphisms are imposed on $\mathbf{L}(\mathbf{y})$ after every I_1 BP iterations for a total of I_2 rounds. Among the candidate hard decisions, the final estimate is selected as the one with the maximum metric. In contrast, PBP abandons the ensemble configuration, applies one automorphism per BP iteration, and triggers early stopping when parity checks are satisfied.

III. MOTIVATIONS AND INITIATIVES

As depicted in Fig. 1, the colored blocks highlight the optimized PCM \mathbf{H}_s and the specific revisions made to the standard NMS decoding.

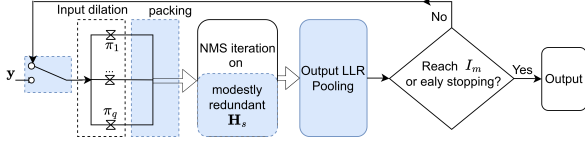


Fig. 1: Block diagram of the revised NMS decoding.

TABLE I: COMPARISON OF ATTRIBUTES OF SELECTED PCMS FOR BCH CODES OF LENGTHS 63 AND 128.

Code	PCM (dimensions)	# of length-4 cycles	Column weight Range/Mean/Std	Row weight Range/Mean/Std	β
(63,36)	$\mathbf{H}(27 \times 63)$ [22]	5909	[1,13] / 7.7 / 3.9	[18,18] / 18 / 0.0	-
	$\mathbf{H}_s(32 \times 63)$	2521	[7,10] / 7.9 / 0.9	[14,16] / 15.3 / 0.9	2
(63,45)	$\mathbf{H}(122 \times 63)$	42724	[27,31] / 29.7 / 1.2	[14,16] / 15.3 / 0.9	20
	$\mathbf{H}(18 \times 63)$ [22]	7251	[1,11] / 6.9 / 2.9	[24,24] / 24 / 0.0	-
	$\mathbf{H}_s(33 \times 63)$	3066	[7,11] / 8.4 / 1.0	[16,16] / 16 / 0.0	2
(127,64)	$\mathbf{H}(78 \times 63)$	19620	[17,21] / 19.8 / 1.0	[16,16] / 16 / 0.0	5
	$\mathbf{H}(63 \times 127)$ [22]	138779	[1,33] / 16.9 / 9.6	[34,34] / 34 / 0.0	-
(127,78)	$\mathbf{H}_s(72 \times 127)$	14900	[10,15] / 12.6 / 1.1	[22,24] / 22.2 / 0.6	2
	$\mathbf{H}(49 \times 127)$ [22]	205240	[1,31] / 17.0 / 8.8	[44,44] / 44 / 0.0	-
(127,78)	$\mathbf{H}_s(57 \times 127)$	24807	[9,15] / 12.6 / 1.1	[28,28] / 28 / 0.0	2

A. Choice of Parity-Check Matrix

Inspired by advancements in LDPC codes, prior studies have primarily focused on reducing the density of the PCM [21], [22], minimizing the count of length-4 cycles in the PCM [5], or increasing row redundancy of the PCM [21]. However, a systematic design methodology that simultaneously incorporates these factors for BCH codes remains absent. This motivated the adaptation of the standard PCM \mathbf{H} through structured row operations.

1) *Optimization Process:* Initialize $S_f = S_g = \emptyset$, $\|\cdot\|$ denotes the Hamming weight. It proceeds as follows:

- 1) Transform \mathbf{H} into its row echelon form \mathbf{H}_r .
- 2) Minimize \mathbf{H}_r 's density through binary additions on rows \mathbf{r}_i and \mathbf{r}_j .


```

for  $i = 1, 2, \dots, M_r$  (number of  $\mathbf{H}_r$ 's rows)
   $w_g = \|\mathbf{r}_i\|$ ;  $S_f \leftarrow \{\mathbf{r}_i\}$ 
  for  $j = 1, 2, \dots, M_r, j \neq i$ 
     $\mathbf{t} = \mathbf{r}_i \oplus \mathbf{r}_j$ 
    if  $\|\mathbf{t}\| = w_g$   $S_f \leftarrow S_f \cup \{\mathbf{t}\}$ 
    if  $\|\mathbf{t}\| < w_g$   $S_f \leftarrow \{\mathbf{t}\}$ ;  $w_g \leftarrow \|\mathbf{t}\|$ 
   $S_g \leftarrow S_g \cup S_f$ 

```

Construct \mathbf{H}_{r1} by combining the unique rows in S_g , excluding duplicates or cyclically shifted versions.

- 3) Perform an exhaustive search iteratively, say $Q = 4$ times:


```

for  $i = 1, 2, \dots, Q$ 
   $\mathbf{H}_r \leftarrow \mathbf{H}_{r1}$ ; Repeat step 2, replacing  $\mathbf{r}_j$  with each of its cyclic shifts  $\mathbf{r}_j^{(q)}$ ,  $q = 1, 2, \dots, N$ .

```
- 4) For the derived \mathbf{H}_{r1} , if its row count $M_{r1} \leq \beta M$ (with β being the redundancy factor), pad it with sorted $\beta(M - M_{r1})$ rows of \mathbf{H}_{r1} in ascending Hamming weight.
- 5) Apply a heuristic method (e.g., simulated annealing) to probabilistically select rows based on their involvement in length-4 cycles, then attempt random cyclic shifts to minimize a loss function that considers the total number of length-4 cycles and the column weight distribution variance. This process yields the final \mathbf{H}_s . ■

Above procedures have been validated for various BCH codes. Partial results are presented in Table I. It demonstrates that the number of length-4 cycles and column weight standard deviation are effectively reduced, even with the imposed row redundancy in \mathbf{H}_s , compared to the original \mathbf{H} .

Table II highlights the FER results for codes denoted as (N, K, M_s) with varying β at SNR = 2.6 dB. Both (63,36) and (63,45) codes exhibit initial FER improvements with increased redundancy, but a turning point arises around $M_s = 122$ and $M_s = 78$, respectively. This suggests that while redundancy benefits FER performance, excessive redundancy introduces additional length-4 cycles, negating the gains. Similar obser-

TABLE II: IMPACT OF VARYING REDUNDANCY FACTOR β OF PCM ON FER PERFORMANCE OF BCH CODES OF LENGTH 63 AT SNR = 2.6DB.

Codes	(63,36,27) / (63,45,18)	(63,36,32) / (63,45,33)	(63,36,72) / (63,45,78)	(63,36,122) / (63,45,108)	(63,36,172) / (63,45,153)
FERs	0.2657/0.1795	0.2495/0.1562	0.175/0.1406	0.1474/0.1767	0.1593/0.2318

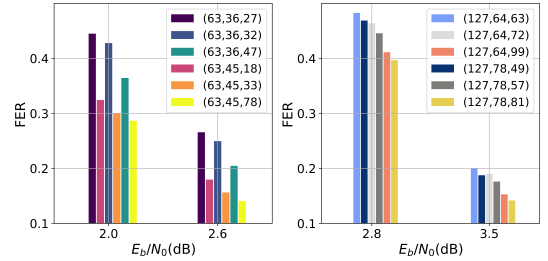


Fig. 2: FER of BCH codes with varying PCM redundancy.

variations hold for the same or other BCH codes at various SNR points, as shown in Fig. 2. (Some higher cases with $\beta > 5$ are omitted for clarity.) It can be seen that an appropriate level of redundancy in \mathbf{H}_s improves FER performance, albeit at the cost of slightly increased computational complexity.

An intriguing and counterintuitive observation can be drawn from Table II and Fig. 2. The (63,45) code demonstrates superior performance compared to the (63,36) code, despite having a comparable number of rows in its PCM. A similar trend is observed for the (127,78) code when compared to the (127,64) code. This phenomenon can be explained by the inability of an \mathbf{H}_s composed solely of minimum-weight rows to achieve a full-rank PCM in GF(2) for the (63,36) or (127,64) codes. As a result, achieving full-rank \mathbf{H}_s for these codes necessitates hybrid Hamming weights, specifically 14/16 and 22/24. Conversely, the (63,45) and (127,78) codes benefit from uniform rows with minimum weights of 16 and 28, respectively, which are sufficient to construct full-rank PCMs. This intrinsic rank deficiency in the (63,36) and (127,64) codes might have been overlooked or underestimated in prior analyses. It is hypothesized that this deficiency plays a critical role in explaining why the higher-rate (63,45) and (127,78) codes, despite having denser PCMs with fewer rows and more length-4 cycles, outperform the (63,36) and (127,64) codes in terms of FER. Notably, above results were obtained under the condition that the revised NMS decoding was employed.

B. Revised NMS Decoder

Since automorphisms of the received sequence \mathbf{y} can be interpreted as different representations of the same transmitted codeword [21], we propose dilating the input by aggregating these representations into an input block $B(\mathbf{y})$. Three types of automorphisms (i.e., permutations) are utilized: Interleaving

π_I , which concatenates bits at even indices with those at odd indices; Frobenius mapping π_F , which maps bit index $i \mapsto 2i \bmod N$; Cyclic shifting π_{C_s} , defined as $s \cdot d_p + d_o \bmod N$, where $d_p = 21, 42$ for length-63, 127 codes respectively, $s \in S_n = \{0, 1, 2\}$, and a random offset $d_o \in [0, d_p)$. For $s \in S_n$, apply π_{C_s} to $S_p = \{\mathbf{y}, \pi_I(\mathbf{y}), \pi_F(\mathbf{y})\}$ individually to yield the $B(\mathbf{y})$ whose size is $|S_n||S_p| = 9$.

Unlike existing iterative decoders for BCH codes, the proposed decoder, as detailed in Algorithm 2 and illustrated in Fig. 1, retains the structure of the original NMS while embedding domain knowledge into the formation of its input.

Algorithm 2 Revised NMS Decoder

Input: Received \mathbf{y} , PCM \mathbf{H}_s , and three types of permutations.

Output: Optimal codeword estimate $\hat{\mathbf{c}}$ for \mathbf{y} .

- 1: **for** $t = 1, 2, \dots, I_m$
- 2: Construct $B(\mathbf{y})$ with shape $|S_n||S_p| \times N$, where $|\cdot|$ denotes set cardinality.
- 3: Perform the variable-to-check message passing in (2) for $B(\mathbf{y})$, followed by the check-to-variable update in (3).
- 4: Reverse the permutations applied to the output of (3), average the results and substitute it for the second term in the RHS of (4) to compute $\mathbf{y}^{(t)}$ and its hard decision $\hat{\mathbf{c}}^{(t)}$.
- 5: **if** $\mathbf{H}_s \hat{\mathbf{c}}^{(t)\top} \neq \mathbf{0}$ **then** update $\mathbf{y} \leftarrow \mathbf{y}^{(t)}$.
- 6: **else break.**
- 7: Return $\hat{\mathbf{c}} = \hat{\mathbf{c}}^{(t)}$.

Compared to PBP or mRRD decoding (as shown in Algorithm 1), the revised NMS replaces BP with NMS in its core operations; three nested iterations are condensed into a single loop with sufficiently small I_m ; multiple permutations applied per iteration. To assess decoding convergence between the revised NMS and standard NMS, we analyzed their performance on the (63,45) code at SNR = 2.6dB, with $\beta = 2$, $I_m = 4$. Both decoders started with the same received sequences, resulting in an initial BER of 0.053 based on hard decisions. The BERs for the revised NMS at the end of each iteration were [0.028, 0.018, 0.015, 0.015], whereas [0.043, 0.040, 0.039, 0.036] for standard NMS. These results clearly indicate that the revised NMS is more effective in accelerating the decoding.

IV. SIMULATION RESULTS AND ANALYSIS

We evaluate four BCH codes: (63,36), (63,45), (127,64), and (127,78) [22]. The revised NMS, henceforth referred to as NMS, is implemented in Python and simulated using the TensorFlow platform. $I_m = 4$ for BCH length-63 codes and $I_m = 8$ for those of length 127. The key parameter α , depending on factors such as the PCM dimensions, input dilation size, and the I_m setting, can be empirically determined at an SNR of 2.6dB for block length 63 and 3.0dB for block length 127. For simplicity, $\beta = 20$ for the (63,36) code while $\beta = 2$ for the other codes, as shown in Table I. We direct interested readers to the open-source code available on GitHub¹ for reproducing results in this work. For consistency, the BER or FER results of the comparison decoders were taken directly from their respective sources rather than re-implementing them.

¹https://github.com/lgw-frank/Short_BCH_Decoding_OSD

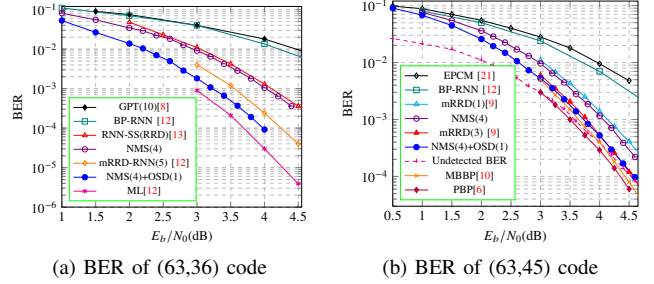


Fig. 3: BER of various decoders for BCH length-36 codes.

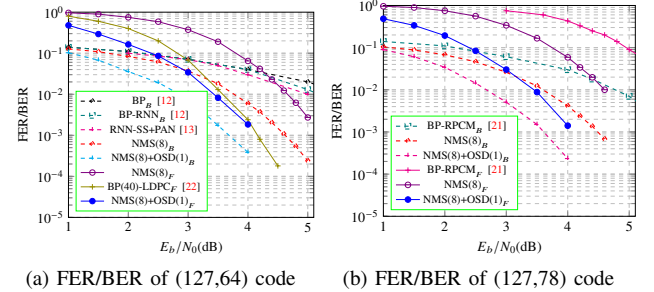


Fig. 4: Performance of decoders for BCH length-127 codes.

1) *Decoding Performance:* For the BCH (63,36) code in Fig. 3a, NMS with $I_m = 4$ slightly outperforms the RNN-SS [13], which adapts RRD by transforming BP into an RNN structure. Moreover, NMS significantly outperforms both the GPT [8] and BP-RNN decoders [12]. In fact, at a BER of 10^{-3} , there is a clear gap of at least 1.5 dB between NMS and the other decoders, as compared with [12, Fig. 8] and Fig. 3a. Although an mRRD with five RNN-neutralized BP subdecoders [12] outperforms NMS by approximately 0.4 dB, this performance gap can be easily bridged by concatenating the latter with order-1 OSD post-processing.

For BCH (63,45) code in Fig. 3b, both the EPCM [21] exploiting circulant PCM and the BP-RNN show inferior performance compared to NMS, highlighting the need for PCM optimization. NMS slightly outperforms the mRRD with one subdecoder, and its combination with order-1 OSD is limited by an undetected BER curve due to false positive decoding, thus performing worse than ensemble decoding schemes such as the mRRD with three subdecoders or MBBP [10]. Meanwhile, PBP [6] achieves the best BER due to its "one permutation per iteration" strategy.

For the longer BCH length-127 codes, the FER metric is denoted with a subscript "F" and the BER metric with a subscript "B." As shown in Fig. 4, NMS outperforms all other iterative decoders significantly in terms of BER. At a BER of 10^{-3} , NMS achieves at least a 1.5 dB improvement over standard BP, BP-RNN, or RNN-SS+PAN [13, Fig.5] for the (127,64) code, as seen in Fig. 4a. Similarly, NMS outperforms BP-RPCM [21, Fig.5] (designed for the (127,71) code) by approximately 1.3 dB at a BER of 10^{-3} for the (127,78) code. A similar trend is observed for FER comparisons. The hybrid NMS and order-1 OSD outperforms NMS alone by approximately 1 dB at FER = 10^{-3} for both codes, suggesting there is significant room for NMS to improve independently.

TABLE III: TYPICAL SETTINGS FOR DECODERS OF BCH (63,45) CODE.

Decoding schemes	Settings			Complexity Ratios
	(I_1, I_2, I_3)	# of permutations per iteration	M_s of PCM	
mRRD(q)[9]	(15,50,q)	1(varied)	18	q
PBP[6]	(15,50,q)	1(varied)	18	q
MBBP[10]	(66,1,3)	1(fixed)	63	0.92
BP-RNN[12]	$I_m = 5$	1(fixed)	18	0.0067
EPCM[21]	$I_m = 5$ (supposed)	1(fixed)	63	0.023
NMS	$I_m = 4$	$ S_n S_p =9$	33	0.088

Interestingly, the performance gap between BP ($I_m = 40$) for LDPC (128,64) code [22] and NMS(8) for BCH (127,64) code does not increase as SNR rises, shown by the similar slopes of the individual curves in Fig. 4a, implying that in the very high SNR region, this gap will eventually close, leaving only the error floor of LDPC codes as the limiting factor.

2) *Complexity Analysis:* Table III summarizes typical parameter settings from the literature for decoders applied to the BCH (63,45) code. In the worst-case scenario, the first three decoders require a total of $I_1 I_2 I_3$ BP iterations per sequence. Specifically, mRRD(q) with q subdecoders in parallel necessitates $750q$ iterations. In contrast, PBP operates similarly to mRRD(q) but in a serial mode. MBBP requires 198 iterations, seemingly less complex; however, the shape of its three PCMs is square, resulting in greater hardware and computational complexity. For BP-RNN and EPCM schemes, their complexity is roughly equivalent to five iterative decodings, though their FER performance is less favorable as shown in Fig. 3. For these schemes, one random permutation or a fixed identity permutation is used for each BP iteration, compared to 9 permutations per NMS iteration on a slightly redundant PCM. The complexity of an iterative decoder is proportional to the product of $|S_n||S_p|$ (# of permutations per iteration), I_m (maximum iterations), and M_s (# of rows of its PCM). We define a complexity ratio as the ratio of the complexity of the current decoder to the benchmark mRRD(1), yielding the varied ratios in the final column of Table III. Compared to mRRD(q), PBP, or MBBP, NMS demonstrates substantially reduced complexity at the cost of a minor performance loss. It also significantly outperforms BP-RDD or EPCM in terms of FER or BER metrics with comparable complexity.

V. CONCLUSION

In this work, we have addressed two key aspects of applying the NMS decoding algorithm to BCH codes. First, the necessity of adapting the standard PCM is demonstrated by introducing appropriate redundancy and eliminating length-4 cycles that arise in its structure. Second, a revised NMS decoder is presented that leverages the cyclic properties of BCH codes, which enhances both decoding performance and convergence speed. Additionally, we have highlighted the challenges posed by rank deficiency, which is inherent to the code structure, as well as the occurrence of false positive decoding in very short BCH codes.

To the best of the authors' knowledge, this work represents the first successful application of parallelizable iterative decoding to high-density parity-check BCH codes, with only a modest increase in operations, such as shifts and binary or real-valued summations.

In the high-SNR regime, to bridge the gap to the ML decoding limit for longer BCH codes while maintaining high

data throughput and reasonable complexity, a hybrid approach combining NMS with OSD shows promise. In this approach, NMS handles the bulk of the decoding workload in parallel, while the OSD is used for serial post-processing of occasional failures left by NMS. This hybrid technique warrants further investigation in future work.

REFERENCES

- [1] R. Gallager, "Low-density parity-check codes," *IRE Trans. Inf. Theory*, vol. 8, no. 1, pp. 21–28, 1962.
- [2] D. J. MacKay and R. M. Neal, "Near shannon limit performance of low density parity check codes," *Electron. Lett.*, vol. 32, no. 18, p. 1645, 1996.
- [3] J. Jiang and K. R. Narayanan, "Iterative soft decoding of Reed-Solomon codes," *IEEE Commun. Lett.*, vol. 8, no. 4, pp. 244–246, 2004.
- [4] —, "Iterative soft-input soft-output decoding of Reed-Solomon codes by adapting the parity-check matrix," *IEEE Trans. Inf. Theory*, vol. 52, no. 8, pp. 3746–3756, 2006.
- [5] T. R. Halford and K. M. Chugg, "Random redundant soft-in soft-out decoding of linear block codes," in *Int. Symp. Inf. Theory*. IEEE, 2006, pp. 2230–2234.
- [6] M. Ismail, S. Denic, and J. Coon, "Efficient decoding of short length linear cyclic codes," *IEEE Commun. Lett.*, vol. 19, no. 4, pp. 505–508, 2015.
- [7] E. Santi, C. Hager, and H. D. Pfister, "Decoding Reed-Muller codes using minimum-weight parity checks," in *Int. Symp. Inf. Theory (ISIT)*. IEEE, 2018, pp. 1296–1300.
- [8] O. P. Babalola, O. Ogundile, and D. J. Versfeld, "A generalized parity-check transformation for iterative soft-decision decoding of binary cyclic codes," *IEEE Commun. Lett.*, vol. 24, no. 2, pp. 316–320, 2019.
- [9] I. Dimnik and Y. Be'ery, "Improved random redundant iterative hdp decoding," *IEEE Trans. Commun.*, vol. 57, no. 7, pp. 1982–1985, 2009.
- [10] T. Hehn, J. B. Huber, O. Milenkovic, and S. Laendner, "Multiple-bases belief-propagation decoding of high-density cyclic codes," *IEEE Trans. Commun.*, vol. 58, no. 1, pp. 1–8, 2010.
- [11] M. Geiselhart, A. Elkelesh, M. Ebada, S. Cammerer, and S. ten Brink, "Automorphism ensemble decoding of Reed-Muller codes," *IEEE Trans. Commun.*, vol. 69, no. 10, pp. 6424–6438, 2021.
- [12] E. Nachmani, E. Marciano, L. Lugosch, W. J. Gross, D. Burshtein, and Y. Be'ery, "Deep learning methods for improved decoding of linear codes," *IEEE J. Sel. Topics Signal Process.*, vol. 12, no. 1, pp. 119–131, 2018.
- [13] M. Lian, F. Carpi, C. Häger, and H. D. Pfister, "Learned belief-propagation decoding with simple scaling and SNR adaptation," in *Int. Symp. Inf. Theory (ISIT)*. IEEE, 2019, pp. 161–165.
- [14] A. Buchberger, C. Häger, H. D. Pfister, L. Schmalen, and A. G. Amat, "Pruning neural belief propagation decoders," in *Int. Symp. Inf. Theory (ISIT)*. IEEE, 2020, pp. 338–342.
- [15] R. Lucas, M. Bossert, and M. Breitbart, "On iterative soft-decision decoding of linear binary block codes and product codes," *IEEE J. Sel. Areas Commun.*, vol. 16, no. 2, pp. 276–296, 1998.
- [16] J. S. Yedidia, J. Chen, and M. P. Fossorier, "Generating code representations suitable for belief propagation decoding," in *Proc. Annu. Allerton Conf. Commun. Control and Comput.*, vol. 40, no. 1. IEEE, 2002, pp. 447–456.
- [17] Y. Kou, S. Lin, and M. P. Fossorier, "Low-density parity-check codes based on finite geometries: a rediscovery and new results," *IEEE Trans. Inf. Theory*, vol. 47, no. 7, pp. 2711–2736, 2001.
- [18] M. P. Fossorier and S. Lin, "Soft-decision decoding of linear block codes based on ordered statistics," *IEEE Trans. Inf. Theory*, vol. 41, no. 5, pp. 1379–1396, 1995.
- [19] M. Bossert, R. Schulz, and S. Bitzer, "On hard and soft decision decoding of BCH codes," *IEEE Trans. Inf. Theory*, vol. 68, no. 11, pp. 7107–7124, 2022.
- [20] L. P. Lugosch, *Learning algorithms for error correction*. McGill University (Canada), 2018.
- [21] M. Baldi, G. Cancellieri, and F. Chiaraluce, "Iterative soft-decision decoding of binary cyclic codes," *J. Commun. Softw. Syst.*, vol. 4, no. 2, pp. 142–149, 2008.
- [22] M. Helmling, S. Scholl, F. Gensheimer, T. Dietz, K. Kraft, S. Ruzika, and N. Wehn, "Database of Channel Codes and ML Simulation Results," www.uni-kl.de/channel-codes, 2019.